$$H = \frac{e}{me}\mathbf{p}\cdot\mathbf{A} + \frac{e^2}{2me^2}\mathbf{A}\cdot\mathbf{A}. \qquad (7.4.3.3)$$

It produces photoelectric absorption through the $\mathbf{p}\cdot\mathbf{A}$ term taken in first order, Compton and Raman scattering through the $\mathbf{A}\cdot\mathbf{A}$ term and resonant Raman scattering through the $\mathbf{p}\cdot\mathbf{A}$ terms in second order.

If resonant scattering is neglected for the moment, the expression for the incoherent scattering cross section becomes

$$S = \sum_f (E_2/E_1)^2 \left| \langle \psi_f | \sum_j \exp(i\mathbf{K}\cdot\mathbf{r}_j) | \psi_i \rangle \right|^2 \delta(E_f - E_i - \Delta E), \qquad (7.4.3.4)$$

where the Born operator is summed over the j target electrons and the matrix element is summed over all final states accessible through energy conservation. In the high-energy limit of $\Delta E \gg E_B$, $S(E_1, E_2, \mathbf{K}, Z) \rightarrow Z$ but as Table 7.4.3.1 shows this condition does not hold in the X-ray regime.

The evaluation of the matrix elements in equation (7.4.3.4) was simplified by Waller & Hartree (1929) who (i) set $E_2 = E_1$ and (ii) summed over all final states irrespective of energy conservation. Closure relationships were then invoked to reduce the incoherent scattering factor to an expression in terms of form factors f_{jk}:

$$S = \sum_j [1 - |f_j(\mathbf{K})|^2] - \sum_j \sum_k^{j \neq k} |f_{jk}(\mathbf{K})|^2, \qquad (7.4.3.5)$$

where

$$f_j(\mathbf{K}) = \langle \psi_j | \exp(i\mathbf{K}\cdot\mathbf{r}_j) | \psi_j \rangle$$

and

$$f_{jk} = \langle \psi_k | \exp[i\mathbf{K}\cdot(\mathbf{r}_k - \mathbf{r}_j)] | \psi_j \rangle,$$

the latter term arising from exchange in the many-electron atom.

According to Currat, DeCicco & Weiss (1971), equation (7.4.3.5) can be improved by inserting the prefactor $(E_2/E_1)^2$, where E_2 is calculated from equation (7.4.3.1); the factor is an average for the factors inside the summation sign of equation (7.4.3.4) that were neglected by Waller & Hartree. This term has been included in a few calculations of incoherent intensities [see, for example, Bloch & Mendelsohn (1979)]. The Waller–Hartree method remains the chosen basis for the most extensive compilations of incoherent scattering factors, including those tabulated here, which were calculated by Cromer & Mann (1967) and Cromer (1969) from non-relativistic Hartree–Fock self-consistent-field wavefunctions. Table 7.4.3.2 is taken from the compilation by Hubbell, Veigele, Briggs, Brown, Cromer & Howerton (1975).

7.4.3.2.2. *Thomas–Fermi model*

This statistical model of the atomic charge density (Thomas, 1927; Fermi, 1928) considerably simplifies the calculation of coherent and incoherent scattering factors since both can be written as universal functions of $\mathbf{K}$ and Z. Numerical values were first calculated by Bewilogua (1931); more recent calculations have been made by Brown (1966) and Veigele (1967). The method is less accurate than Waller–Hartree theory, but it is a much simpler computation.

7.4.3.2.3. *Exact calculations*

The matrix elements of (7.4.3.4) can be evaluated exactly for the hydrogen atom. If one-electron wavefunctions in many-electron atoms are modelled by hydrogenic orbitals [with a suitable choice of the orbital exponent; see, for example, Slater (1937)], an analytical approach can be used, as was originally proposed by Bloch (1934).

Table 7.4.3.3. *Compton scattering of Mo Kα X-radiation through 170° from 2s electrons*

Element	$S_{\rm exact}$	$S_{\rm imp}$	$S_{\rm W-H}$
Li	0.879	0.878	0.877
B	0.879	0.878	0.877
O	0.878	0.877	0.876
Ne	0.875	0.875	0.875
Mg	0.863	0.863	0.872
Si	0.851	0.850	0.868
Ar	0.843	0.826	0.877
V	0.663	0.716	0.875
Cr	0.568	0.636	0.875

$S_{\rm exact}$ is the incoherent scattering factor calculated analytically from a hydrogenic atomic model. $S_{\rm imp}$ is the incoherent scattering factor calculated by taking the Compton profile derived in the impulse approximation and truncating it for $\Delta E < E_B$. $S_{\rm W-H}$ is the Waller–Hartree incoherent scattering factor. Data taken from Bloch & Mendelsohn (1974).

Hydrogenic calculations have been shown to predict accurate K- and L-shell photoelectric cross sections (Pratt & Tseng, 1972). The method has been applied in a limited number of cases to K-shell (Eisenberger & Platzman, 1970) and L-shell (Bloch & Mendelsohn, 1974) incoherent scattering factors, where it has served to highlight the deficiencies of the Waller–Hartree approach. In chromium, for example, at an incident energy of ~ 17 keV and a Bragg angle of 85°, the L-shell Waller–Hartree cross section is higher than the 'exact' calculation by $\sim 50\%$. A comparison of Waller–Hartree and exact results for 2s electrons, taken from Bloch & Mendelsohn (1974), is given in Table 7.4.3.3 for illustration. The discrepancy is much reduced when all electrons are considered.

In those instances where the exact method has been used as a yardstick, the comparison favours the 'relativistic integrated impulse approximation' outlined below, rather than the Waller–Hartree method.

7.4.3.3. *Relativistic treatment of incoherent scattering*

The Compton effect is a relativistic phenomenon and it is accordingly more satisfactory to start from this basis, *i.e.* the Klein & Nishina (1929) theory and the Dirac equation (see Jauch & Rohrlich, 1976). In second-order relativistic perturbation theory, there is no overt separation of $\mathbf{p}\cdot\mathbf{A}$ and $\mathbf{A}\cdot\mathbf{A}$ terms. The inclusion of electron spin produces additional terms in the Compton cross section that depend upon the polarization (Lipps & Tolhoek, 1954); they are generally small at X-ray energies. They are of increasing interest in synchrotron-based experiments where the brightness of the source and its polarization characteristics compensate for the small cross section (Blume & Gibbs, 1988).

Somewhat surprisingly, it is the spectral distribution, $\mathrm{d}^2\sigma/\mathrm{d}\Omega\,\mathrm{d}E_2$, rather than the total intensity, $\mathrm{d}\sigma/\mathrm{d}\Omega$, which is the better understood. This is a consequence of the exploitation of the Compton scattering technique to determine electron momentum density distributions through the Doppler broadening of the scattered radiation [see Cooper (1985) and Williams (1977) for reviews of the technique]. Manninen, Paakkari & Kajantie (1976) and Ribberfors (1975) have shown that the

Compton profile – the projection of the electron momentum density distribution onto the X-ray scattering vector – can be isolated from the relativistic differential scattering cross section within the impulse approximation. Several experimental and theoretical investigations have been concerned with understanding the changes in the spectral distribution when electron binding energies cannot be discounted. It has been found (*e.g.* Pattison & Schneider, 1979; Bloch & Mendelsohn, 1974) that, to a high degree of accuracy, the spectral distribution is merely truncated at energy transfers $E \leq E_B$.

This has led to the suggestion that the incoherent intensity can be obtained by integrating the spectral distributions, *i.e.* from

$$\frac{\mathrm{d}\sigma}{\mathrm{d}\Omega} = \int_{E_1 - E_B}^{\infty} \frac{\mathrm{d}^2\sigma}{\mathrm{d}\Omega\,\mathrm{d}E_2}\,\mathrm{d}E_2. \qquad (7.4.3.6)$$

Unfortunately, this requires the Compton profile of each electron shell as input [Compton line shapes have been tabulated by Biggs, Mendelsohn & Mann (1975)] for all elements.

Ribberfors (1983) and Ribberfors & Berggren (1982) have shown that this calculation can be dramatically simplified, without loss of accuracy, by crudely approximating the Compton line shape. Fig. 7.4.3.2 shows the incoherent scattering from aluminium, modelled in this way, and compared with experiment, Waller–Hartree theory, and an exact integral of the truncated impulse Compton profile.

7.4.3.4. *Plasmon, Raman, and resonant Raman scattering*

In typical X-ray experiments, as is evident from Table 7.4.3.1, the energy transfer may be so low that Compton scattering will be inhibited from all but the most loosely bound electrons. Indeed, in the situation in metals where $\mathbf{K}$, the momentum transfer, is less than $\mathbf{k}_F$ (the Fermi momentum), Compton scattering from the conduction electrons may be restricted by exclusion because of the lack of unoccupied final states [see Bushuev & Kuz'min (1977)]. Fortunately, in these uncertain circumstances, the incoherent intensities are low. In this regime, the electron gas may be excited into collective motion. For almost all solids, the plasmon excitation energy is 20–30 eV and, in the random phase approximation, the incoherent scattering factor becomes $S(\Delta E, K) \propto (K^2/w_p)\delta(\Delta E - h\omega_p)$, where ω_p is the plasma frequency.

At slightly higher energies ($\Delta E \geq E_B$), Compton scattering and Raman scattering can coexist, though the Raman component is only evident at low momentum transfer (Bushuev & Kuz'min, 1977). The resultant spectrum is often referred to as the Compton–Raman band. In semi-classical radiation theory, Raman scattering is usually differentiated from Compton scattering by dropping the requirement for momentum conservation between the photon and the individual target electron, the recoil being absorbed by the atom. The Raman band corresponds to transitions into the lowest unoccupied levels and these can be calculated within the dipole approximation as long as $|\mathbf{K}|a < 1$, where $\mathbf{K}$ is the momentum transfer and a the orbital radius of the core electron undergoing the transition. The transition probability in equation (7.4.3.4) becomes

$$\sum_f |\langle\psi_f|\mathbf{r}|\psi_i\rangle|^2 \delta(E_f - E_i - \Delta E), \qquad (7.4.3.7)$$

which implies that the near-edge structure is similar to the photoelectric absorption spectrum.

Whereas plasmon and Raman scattering are unlikely to make dramatic contributions to the total incoherent intensity, resonant Raman scattering (RRS) may, when $E_1 \leq E_B$. The excitation involves a virtual K-shell vacancy in the intermediate state and a vacancy in the L (or M or N) shell and an electron in the continuum in the final state. It has now been observed in a variety of materials [see, for example, Sparks (1974), Eisenberger, Platzman & Winick (1976), Schaupp *et al.* (1984)]. It was predicted by Gavrila & Tugulea (1975) and the theory has been treated comprehensively by Åberg & Tulkki (1985). The effect is the exact counterpart, in the inelastic spectrum, of anomalous

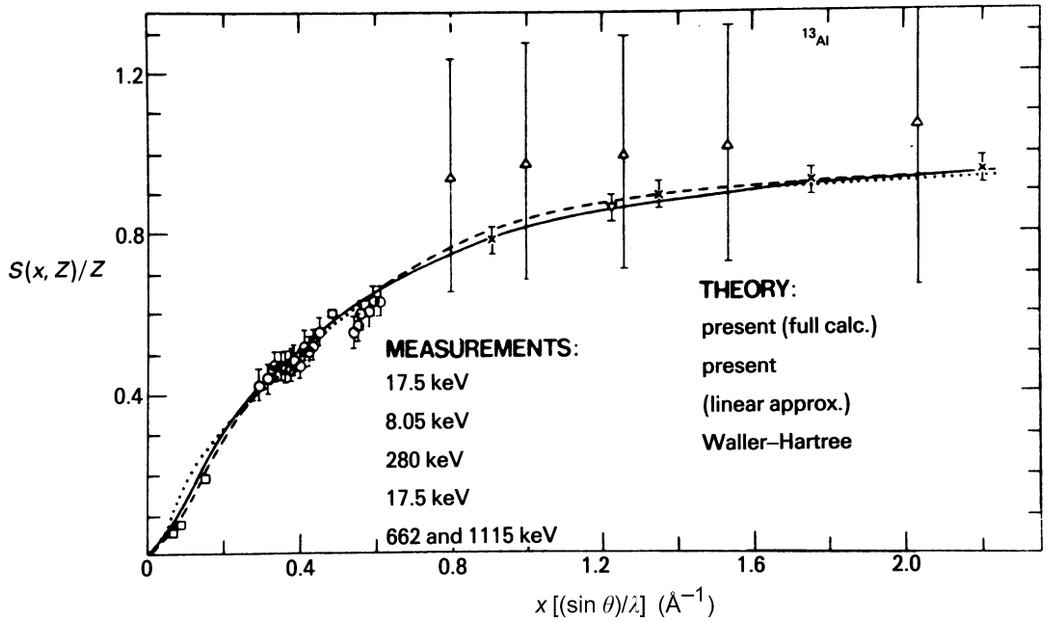

Fig. 7.4.3.2. The incoherent scattering function, $S(x, Z)/Z$, per electron for aluminium shown as a function of $x = (\sin\theta)/\lambda$. The Waller–Hartree theory (·····) is compared with the truncated impulse approximation in the tabulated Compton profiles (Biggs, Mendelsohn & Mann, 1975) cut-off at $E < E_B$ for each electron group (——). The third curve (– – –) shows the simplification introduced by Ribberfors (1983) and Ribberfors & Berggren (1982). The predictions are indistinguishable to within experimental error except at low $(\sin\theta)/\lambda$. Reference to the measurements can be found in Ribberfors & Berggren (1982).

references